PROCEEDINGS, 51st Workshop on Geothermal Reservoir Engineering
Stanford University, Stanford, California, February 9-11, 2026
SGP-TR-230

Application of the CSTR in Series Model on Geothermal Tracer Returns to Evaluate Long-term Reservoir Temperature Stability

Nicholas Silva, John Murphy, and Adam Johnson

6884 Sierra Center Pkwy, Reno, NV, 89511

nsilva@ormat.com

Keywords: tracer, reinjection, recycling, temperature forecast

ABSTRACT

Tracer studies in geothermal fields help quantify injection returns to production and can help predict thermal breakthrough. Often these returns are convoluted with the recycling associated with reinjection and require deconvolution to interpret the single-pass performance. The deconvolution technique discussed in this paper uses the CSTR in Series model, which is a simple model often applied in reactor design engineering for non-ideal residence time distribution analysis. A key advantage of the CSTR in Series model is its simple Laplacian transfer function which provides an analytical solution for impulse disturbances, such as tracer injection, regardless of the number of passes through the system. When applied to a geothermal system, the transfer functions between each injector-producer pair, or a field-average transfer function, can be determined and a temperature forecast can be created by introducing a step-change disruption to the transfer functions. An empirical correlation to re-scale the CSTR time parameter of the transfer function is being evaluated to improve temperature forecasts and better account for heat in place.

1. INTRODUCTION

Geothermal power plants utilize the natural hot fluid found below the Earth's surface to generate electricity, but they require a large flow throughput. A local reinjection strategy can provide pressure support to production and dispose of the cooled brine, but one of the major challenges is identifying a balance between the pressure and temperature decline. If the reinjection communicates too much with production, the resource may undergo significant temperature decline and reduce generation (Forest, 1995), but if the brine is reinjected in a location with little communication with production, the resource may undergo dramatic pressure declines which may result in pulling non-geothermal fluids into the system and still cool the resource (Benoit, 1997). Fortunately, an improved production and injection strategy can result in reduced temperature declines (Benoit, 2017) and potentially some temperature recovery as seen at the Stillwater Geothermal Plant (Forest, 1995).

Tracer studies are crucial tests to determine the residence time distribution (RTD) associated with reinjection returns. By determining how much and how quickly the tracer returns to production, one could estimate how reinjection affects production temperatures over time. There are numerous methods of analyzing tracer returns to make various conclusions about the reservoir, such as determining mean residence times, estimating reservoir geometries (Shook, 2003), or implementing of a convective-dispersion model (Horne, 1985), but analysis relies on a properly conducted tracer test. In practice, tracer tests come with various challenges.

The ideal tracer for a geothermal test must be water-soluble, inert, conservative, and measurable at low concentrations (Shook, 2004). Naphthalene sulfonate tracers have demonstrated success as a geothermal tracer, although degradation reactions may occur at reservoir temperatures >200°C (Sajkowski, 2021) or >310°C (Rose, 2001) depending on the selected tracer. The thermal degradation can be estimated using the Arrhenius equation (Levenspiel, 1972) and known kinetics for the tracer. The tracer must be introduced in a manner that is quick and well-mixed with the reinjectate. Operation also introduces some additional challenges. Most RTD analysis techniques, much like the methods discussed in this paper, require steady operation throughout the test as any changes in injection or production would affect the conditions in the reservoir. Another operational challenge is interpreting the measured tracer profile with the recycling observed from production to injection. A tracer injected into a specific injector and measured at a specific producer focuses on that connection but also contains undesired effects from all the possible forms of recycling associated with other producers and injectors. This creates a large network of intertwined recycling loops and convolutes the measured data from the true single-pass tracer returns.

The method of moments described by Shook (2005a, 2005b) is a powerful and simple method to deconvolute tracer data assuming the reinjection profile is equal to the combination of the single-pass returns profile and the Dirac delta function associated with the initial tracer injection. It can be used to estimate individual injector to producer pathways or a field-wide average return profile but the described method only deconvolutes assuming a single recycle, so it does not fully deconvolute the long tracer tail. Depending on the type of tracer analysis, such as investigating first returns or peak returns, the complete deconvolution of late time may be unnecessary; however, when investigating total tracer returns, it is often better to deconvolute all recycle loops and prevent overestimation.

The tracer modeling methods discussed in this paper use the Laplacian transfer functions associated with continuously stirred tank reactors (CSTRs) and plug flow reactors (PFRs) to form a network between injection and production. CSTRs and PFRs are two simple and ideal models implemented in reactor design engineering and may have different terms in the geothermal industry. The basics are described in more detail in Section 2. The CSTR in Series model, sometimes referred to as the Tanks in Series model (TiS), is often used for RTD

analysis to empirically represent non-ideal reactors (Toson, 2019; Cherkasov, 2023). The approach discussed in this paper uses their simple Laplacian transfer functions to deconvolute infinite recycling and cross-well reinjection during geothermal operation. Early tracer papers in the geothermal industry have considered the TiS model for RTD analysis to represent field data with mixed degree of success (Robinson, 1982; Tester, 1986), but it appears to be scarcely considered currently.

This paper introduces the basics of the Laplacian transfer functions associated with TiS model and implements it for a geothermal system to assess how geothermal operation and recycling affect the tracer returns. The results of the TiS model are then used to assess how the injection returns affect the production temperatures. More advanced implementations of the transfer function network are introduced but are not evaluated against field data.

2. THEORY

This section introduces the basic principles associated with the TiS model and how it is used to represent injection return pathways in a geothermal system.

2.1 CSTR and PFR basics

The basics of CSTRs and PFRs are commonly found in introductory chemical engineering reactor design textbooks, such as Levenspiel (1972) or Fogler (2014). A CSTR assumes perfect mixing and infinite dispersion, meaning that every unit of space within the tank has the same concentration across all time. When something enters the tank at a higher concentration, it is instantly and uniformly distributed across the volume. The simplified mass balance is as follows

$$V\frac{dc}{dt} = c_0 Q - cQ - R \tag{1}$$

where V is the volume of the CSTR, c is the concentration in the CSTR, c_0 is the concentration entering the CSTR, Q is the volumetric flow rate through the CSTR, t is time, and R is the mass generation term, typically associated with chemical reactions. In the case of an inert chemical, like an ideal tracer, the generation term is zero. The equation is frequently represented by replacing V/Q with the residence time, τ. The simplified representation for an inert tracer through a CSTR follows

$$\tau\frac{dc}{dt} + c = c_0 \tag{2}$$

A plug flow reactor (PFR) is summarized as a series of plugs extending in an axial direction, or a pipe with uniform concentration in the radial direction, but zero dispersion axially. A series of PFRs is simply a larger PFR. Since there is no dispersion in the direction of flow, the residence time distribution is a Dirac delta function.

Both a CSTR and PFR represent ideal systems; however, imperfect or real residence time distributions can be modeled by incorporating a series of CSTRs as shown in Figure 1. As the number of CSTRs increase, n, the modeled dispersion decreases and as it approaches infinity, the concentration profile resembles a PFR with a residence time equal to the cumulative residence time of the CSTRs. Incorporating a PFR into the model slides the concentration profile through time without affecting the degree of dispersion.

Although the physical meaning of a series of CSTRs suggest the number of tanks must be an integer value, the empirical model uses fractions of CSTRs. It is important to note that the number of CSTRs and residence time of each CSTR independently affects the concentration profile. The outlet concentration profile of 3.5x 10-hour CSTRs differs from the profile of 3x 10-hour CSTRs and 1x 5-hour CSTR. More complicated systems can be modeled with different residence times for each CSTR; however, an analytical concentration equation can be obtained if all the CSTRs in series have the same residence time.

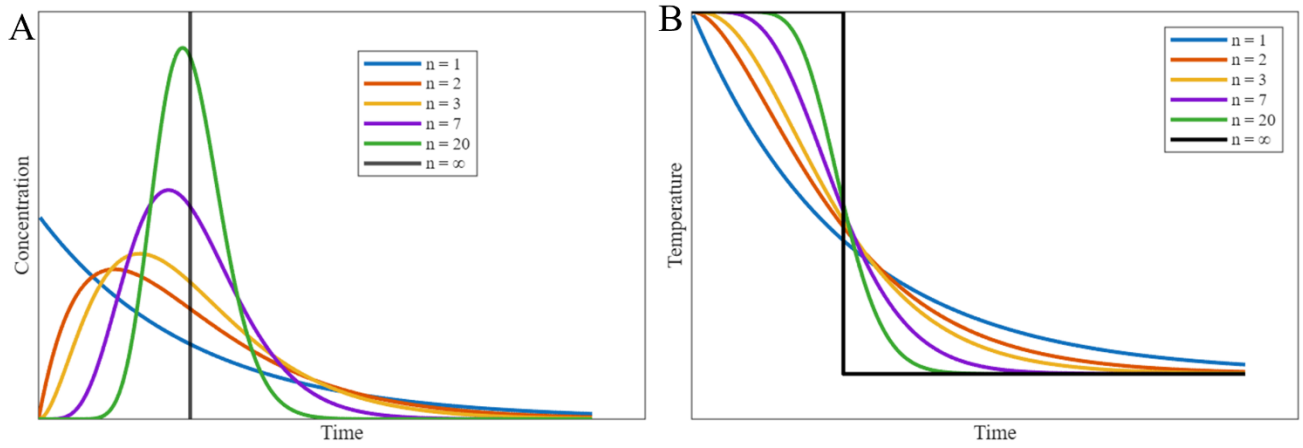

Figure 1: Example (A) concentration profiles after an impulse disturbance and (B) temperature profiles after a step-rate disturbance for different numbers of CSTRs (n) in series. The cumulative residence time of the series of the CSTRs is constant.

2.2 Laplacian transfer functions

Laplacian transfer functions are often used for process controls and are useful for determining the transient effects of a system after a disturbance (Romagnoli, 2012). The advantage to the CSTR and PFR models is their simple representation in Laplacian space, which is accompanied by direct, analytical functions in time. For example, when injecting a tracer, the concentration disturbance would resemble a Dirac delta function and when applied to a simple CSTR and PFR model, the resulting profile has an analytical solution. The effect of *n* on the outlet concentration profile is shown in Figure 1A.

In the case of cold reinjection, the temperature disturbance would resemble the Heaviside function, or a step change. This disturbance upon the CSTR/PFR model does not have an analytical solution and needs to be numerically solved (Abate, 2006). The transient effects of *n* on the outlet temperature with a colder fluid sweeping through the system is shown in Figure 1B. The respective transfer functions and disturbances are summarized using the Laplacian variable, *s*, in Table 1.

Table 1: Laplacian transfer functions and disturbances.

Model Component	Transfer Function (Laplacian space)
CSTR	$\frac{1}{\tau s + 1}$
PFR	$e^{-\tau s}$
Junction	r
Impulse disturbance	1
Step disturbance	$\frac{1}{s}$

2.3 Reservoir model

The basic geothermal reservoir model applied for this study is depicted in Figure 2 with (A) representing a cross section of San Emidio, an operating geothermal system (Folsom, 2020), and (B) serving as the simplified, nodal representation. Often, geothermal operation produces near the upflow and reinjects near an outflow (Figure 2A); in the nodal representation (Figure 2B), some of the reinjectate will leave the system through the outflow and the returning reinjectate will pass through the empirical fit of PFRs and CSTRs and get diluted with the upflow at a recycle fraction, *r*. Note that this simplified model does not include production pulling from proximal fluids, ex: non-geothermal fluids or other outflows. In such cases, *r* would be relative to all other fluid sources; the reinjection return conclusions will be similar, but the estimated production temperatures would be impacted since there are other significant cooling mechanisms.

When the individual transfer functions are combined for an *n* number of CSTRs, the total function through the modeled reservoir is

$$T_1(s) = \frac{c_{out}(s)}{c_{in}(s)} = re^{-\tau_p s}\left(\frac{1}{\tau_c s + 1}\right)^n \tag{3}$$

The subscripts *p* and *c* on the residence time correspond to the PFR and CSTRs, respectively. After introducing the impulse disturbance associated with injecting the tracer, the concentration profile through time, *t*, follows

$$c_{out}(t) = \frac{r}{\tau_c^n * \Gamma(n)}\left((t-\tau_p)^{n-1}\exp\left(-\frac{t-\tau_p}{\tau_c}\right)\right) H(t-\tau_p) \tag{4}$$

Where Γ represents the gamma function and *H* represents the Heaviside function. This form resembles other TiS representations (Toson, 2019; Cherkasov, 2023) but also includes the time skew associated with the PFR and the dilution factor. Since the gamma function and exponents grow rapidly, it is often more computationally efficient to calculate the results in log space using the log gamma function $\Gamma_{\log}$.

$$c_{out}(t) = \mathrm{r} * \exp\left((n-1) * log(t-\tau_p) - \Gamma_{log}(n) - (n) * log(t_c) - \frac{t-\tau_p}{\tau_c}\right) H(t-\tau_p) \tag{5}$$

The outlet concentration profile is non-unique as it's the same regardless of the order of the CSTRs or PFRs. As such, assumptions or more advanced models relying on other sources of data are needed to extrapolate the results to a different operating condition from the one during the tracer test.

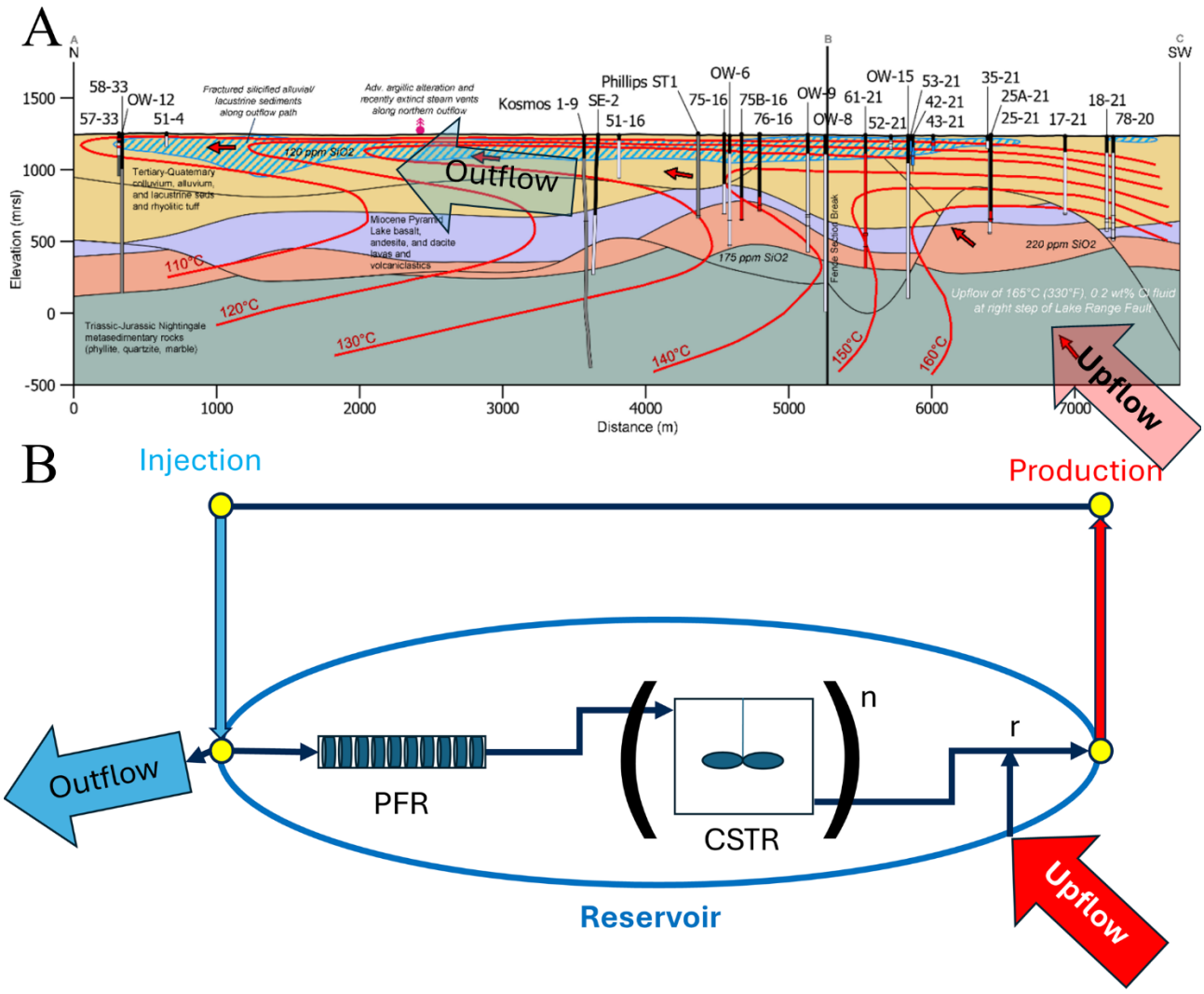

Figure 2: (A) Example conceptual model cross section for San Emidio (Folsom, 2020) with (B) a simplified reservoir diagram represented as a PFR, a series of CSTRs, and a junction with the resource upflow.

3. APPROACHES TO RECYCLING

This section discusses some different approaches used to deconvolute the tracer measurements from recycling. In each circumstance it is important to implement proper measurement corrections (ex: purity, flash, degradation) and normalize the tracer profile to the mass of tracer injected and the production flow rates so that the total tracer mass returns are unitless.

3.1 Method of moments

As previously stated, the method of moments (MoM) deconvolution technique is a powerful and simple method to deconvolute recycling. The method is more completely described by G. Shook (2005a), with the deconvolution equation for 100% reinjection summarized below

$$E(t) = E_{app}(t) - \int_0^t E(t-\tau)E(\tau)d\tau \tag{6}$$

where E(t), is the normalized, single-pass, concentration profile, and $E_{app}(t)$ is the normalized, measured tracer profile convoluted by recycling. The method is generally accurate around the peak tracer profile if the data is reliable. The described method only deconvolutes a single recycle loop of the same RTD, so it is best used for cases where the total reinjection returns are small and the geothermal field is homogenous.

The primary advantages to the methods discussed in the following sections are the ability to deconvolute continuous recycling and implement cross-recycle connections; however, both methods require tuning a model to fit the data rather than reevaluating the data forward through time. Preliminary model parameters can be obtained by regressing Eq. 5 to the early-time, normalized tracer profile

deconvoluted using MoM. The recommended time limit is the average residence time because after this time, the effects of the second and subsequent recycle loops become more prominent.

3.2 Looped evaluation of transfer functions

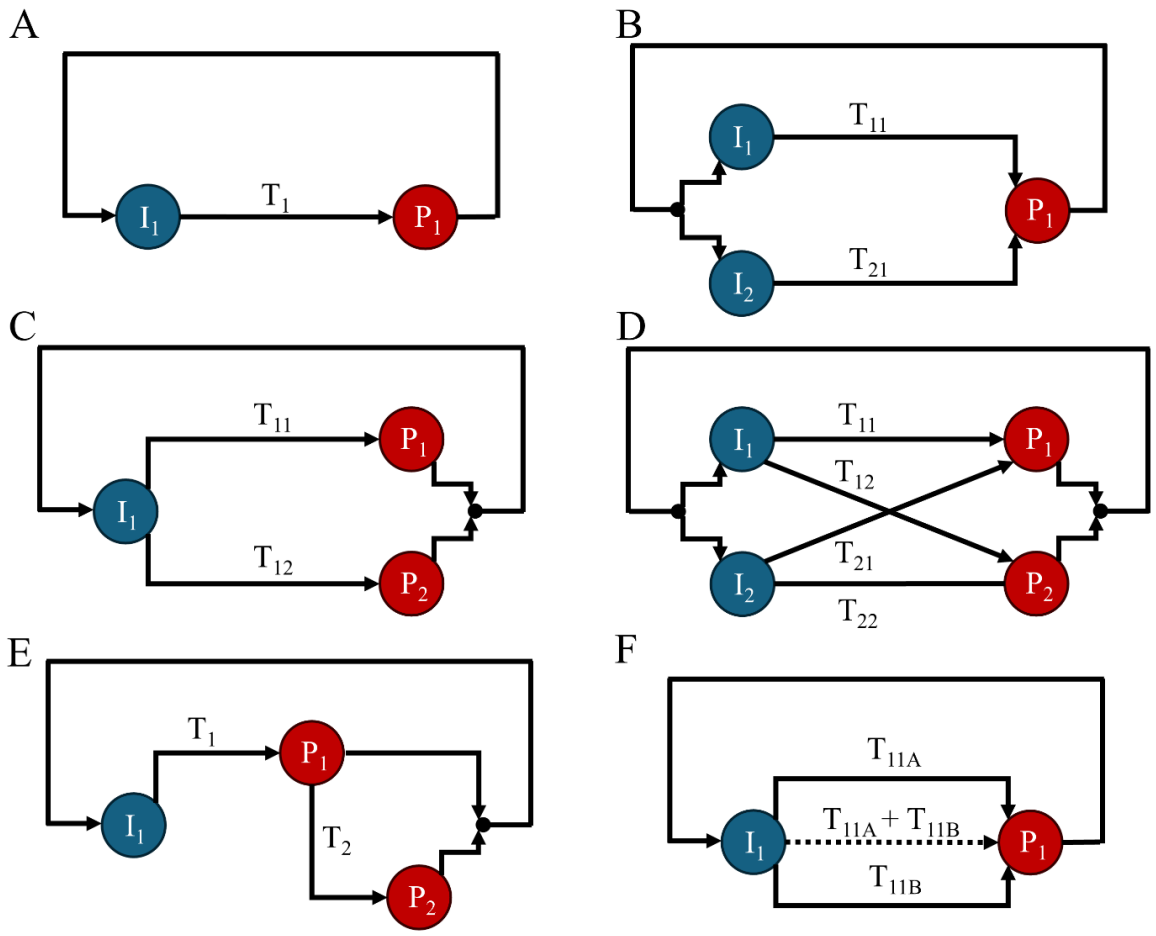

Figure 3: Types of reservoir model and transfer function simplifications for a geothermal system: (A) field-averaged or 1 injector to 1 producer, (B) production-averaged or multiple injectors to 1 producer, (C) injection-averaged or 1 injector to multiple producers, (D) independent transfer functions of multiple injectors to multiple producers, (E) a variation of C with non-independent pathways, and (F) a variation of A where there are two different pathways between an injector or producer.

The looped evaluation transfer function method is a quantitatively more rigorous at deconvoluting but is more versatile as it can be applied to multiple pathways. Figure 3 summarizes some of the various ways to approximate a geothermal reservoir. Figure 3A is the simplest representation of the reservoir by averaging its performance as a single injector to single producer pathway. This approximation has been adequate for most Basin and Range geothermal systems that harness and reinject around a single upflow (e.g. Beowawe and Brady, in current operation). Figure 3B represents multiple injectors traveling to a single, averaged producer (e.g. Tuscarora, Tungsten Mountain). This orientation is more applicable if there are two or more distinct pathways between injection and production, the geothermal field is harnessing one upflow, and the individual performance of each injection pathway is important to quantify. Figure 3C represents an averaged injection returning to multiple producers. For a geothermal system, this is best applied if a field is harnessing two or more unique reservoir zones, but injection is clustered between them (e.g. Dixie Valley and Mammoth). Figure 3D represents an unsimplified reservoir where the pathways between each injector and producer pair is assessed but each pathway is assumed independent from each other. Figure 3E is an example of a simplified reservoir trying to remove some of the pathway independence. This model can be used to estimate a geothermal system where there are two producers, one close and one far from injection, and it is believed that most of the returns to the distal producer follow the same pathway up to the close producer. Figure 3F is a variation of Figure 3A where a single injector has two unique pathways to a producer. Since the inputs and outputs are the same nodes, the overall transfer function can be written as the sum of the independent pathways as represented by the dotted arrows (Romagnoli, 2012). The models in Figure 3A, C, and E each make different assumptions and can be used on the same geothermal system as a type of uncertainty to estimate how the reservoir would perform at different operating conditions. In practice, it is best to use a simpler model to represent the data since each transfer function introduces four new variables for the model (τ_c, τ_p, n, and r). Most of this paper focuses on the model presented in Figure 3A, which mimics the geothermal representation in Figure 2B.

The total transfer function described in Eq. 3 represents the concentration response when passing through the reservoir once, but it can be expanded to the *i*-th loop by passing through the total transfer function *i* times. The general formula for the *i*-th response follows

$$T_i(s) = \frac{dc_{in}(s)}{dc_{out}(s)} = r^i e^{-i\tau_p s}\left(\frac{1}{\tau_C s + 1}\right)^{in} \tag{7}$$

Thus, the tracer return profile would resemble the superimposition of all the recycles. The convoluted transfer function, T_r, associated with the recycle loops is

$$T_r(s) = \sum_{i=1}^{\infty} r^i e^{-i\tau_p s}\left(\frac{1}{\tau_C s + 1}\right)^{in} \tag{8}$$

For the cases where the residence time of all the CSTRs have the same τ_c, each index of the summation transforms into an analytical solution, so it is not numerically rigorous. Depending on the duration of the tracer test, and the recycle fraction, only the first 2-5 indices of the summation make a significant difference for the convoluted response.

The same principles can be applied to more complicated models consisting of multiple pathways (ex: Figure 3B-E); there needs to be extra caution with the flow normalization constants for the different production or injection transfer functions and including all possible ways the injected tracer can reach the selected producer through the recycle loops.

3.3 Transfer function with recycle loop

For the simpler models, an overall transfer function can be obtained through simplifying the recycle loop. A block diagram following the Figure 3A and Figure 3F (with $T_1 = T_{11A} + T_{11B}$) recycle loop can be simplified to the overall, convoluted transfer function

$$T_{1,r}(s) = \frac{T_1(s)}{1 - T_1(s)} \tag{9}$$

T_1 follows Eq 3. There is no analytical solution for this expression using the TiS model, so it must be numerically calculated. If there are multiple injectors to singular production pathways (Figure 3B), the simplified convoluted transfer function for Injector 1 can be written as

$$T_{1,r}(s) = \frac{T_1(s)}{1 - \sum x_j * T_j(s)} \tag{10}$$

where the *j* summation index denotes the injector and x_j is the fraction of flow sent to injector *j*. The models shown in Figure 3C-E which include multiple producers become multivariate transfer functions and determining a simplified loop expression was outside the scope of the paper.

4. MODEL EXAMPLES

4.1 Ideal example

This section describes a simple, ideal reservoir example consisting of two injectors (I1 and I2) and one producer (P1) and walks through how the various approximations and deconvolution techniques affect an approximated single-pass profile. The data was created following the model presented in Figure 3B where the single-pass profiles perfectly match a TiS model with parameters summarized in Table 2.

Table 2: Model parameters used for the ideal recycling example.

Well	Flow Rate [kg/s]	Recycle Fraction	# of CSTRs	Total CSTR time [d]	PFR Time [d]
I1	300	0.6	3	60	3
I2	200	0.4	1.9	40	5
Averaged	500	0.5212	2.47	54.69	3.15
I1 Fit		0.5656	3.555	57.59	1.136
I2 Fit		0.4415	1.446	46.49	7.291

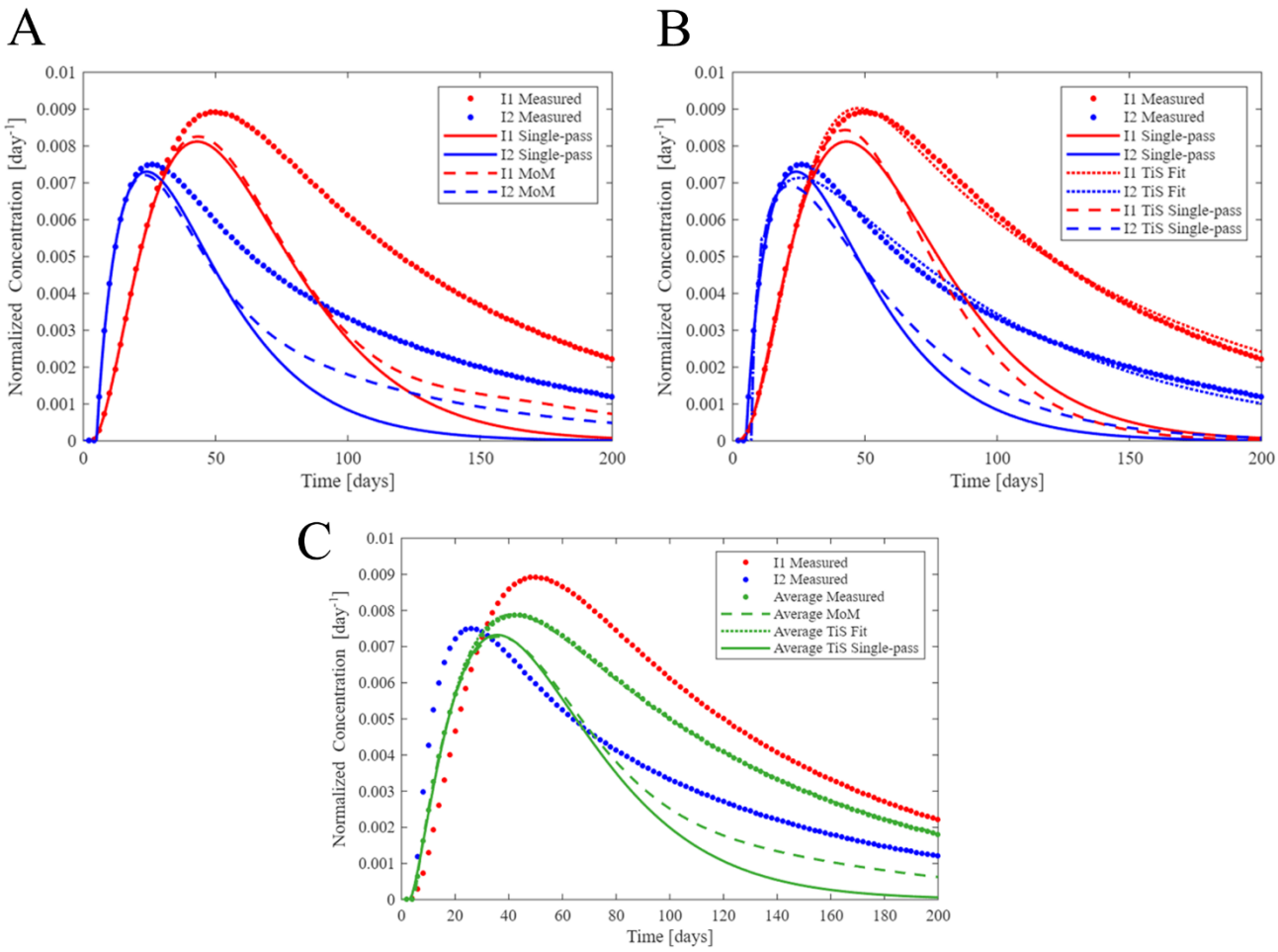

Figure 4: Deconvolution techniques of an ideal system with two injectors and one producer. The measured tracer profiles are created following the model in Figure 3B with the operational parameters in Table 2. (A) Shows the MoM deconvolution of the measured profile. (B) Shows the best-fit TiS model for the measured profiles but assumes no cross recycling. (C) Shows both deconvolution techniques on the field-average measured profiles.

The tracer profiles in Figure 4A summarizes the MoM deconvolution from the measured profiles. The deconvolution is strong for early time data with only slight differences compared to the true single-pass profile. I1 is slightly overestimated because some of the recycling goes to I2, which has a lower recycling fraction. The opposite is seen for I2. In general, the fit is accurate enough relative to measured data. The main concern occurs at late time, where the long tail is not fully deconvoluted. The deviation begins roughly around 1.5*cumulative CSTR residence times and will lead to overpredicting the single-pass cumulative tracer returns. This parameter appears to have a significant impact on the magnitude of production temperature declines and is discussed in more detail in Section 5.

The deconvolution technique in Figure 4B is trying to fit the simple TiS model (Figure 3A) to the measured profile, even though there is cross recycling. The best fit parameters with the least squared residuals from data, are summarized as the I1 Fit and I2 Fit in Table 2. In general, the fit is rudimentary, particularly for an ideal example, since it does not fully grasp the measured profiles for either injector which may be why the model was not previously recommended to use on geothermal systems (Tester, 1986). The best fit parameters do not match the true values; the recycling fraction and total CSTR time skew towards the average value, and the # of CSTRs and PFR time skew away from the average to compensate. The fit can be used to roughly represent the tracer and, most importantly, the cumulative profile, but the MoM deconvolution is more accurate for peak times and performance. A better reservoir model needs to be implemented to improve the TiS fit. For example, the model in Figure 3B would return the exact input parameters back, or the injection performance can be averaged to obtain a field-wide average performance.

Figure 4C summarizes the field-averaged returns. The measured I1 and I2 tracer returns were weighted by the injection rate to obtain a field-weighted average of the measurements. This profile was deconvoluted using the MoM and the best-fit TiS model. Both deconvolution techniques agreed to a high degree for the early time single-pass performance. The main discrepancy is the long-tail which affects the single-pass tracer mass returns. The single-pass profiles begin to diverge around 60 days, which is roughly the average residence time and when the second recycle loop begins to have a larger effect. On the presented time scale, the cumulative tracer returns for the TiS method is 0.52 and the MoM is 0.60, showing MoM would slightly overestimate injection connectivity.

The field averaging approximation transformed the data in a way that made both deconvolution methods agree for early time and the best-fit TiS parameters nearly equaled the input average. A small amount of error was introduced as the best-fit recycle fraction was 0.5212, but the weighted average is 0.52; however, this approximation accurately portrayed the system in four variables instead of eight and can provide insight for how the field performs on average. If the test was conducted for infinite time, the best-fit recycle fraction converges to the true value of 0.52. Since that is impractical, test durations longer than twice the average single-pass residence time tend to give reasonable estimates, but accuracy improves for longer tests.

4.2 Field example - Tuscarora

Real data has more variation than the ideal scenarios presented in Section 4.1, so in this section, the MoM and TiS deconvolution techniques were used on a real tracer study conducted in Tuscarora in 2020 (Kluge, 2025). At the time of the tracer test, there were four active producers (35A-8, 65A-8, 65B-8, and 65-C) and four injectors (53-8, 66-5, 66A-5, and 87A-5), but most of the returns were associated with IW 53-8. The tracer test was nearly fully specified. Three unique sulfonate tracers (PTSA; 2-NSA; 1,3,5-NTSA) were injected into three injectors (not 66A-5), and the returns were measured at all producers. It was assumed these tracers did not degrade at the resource temperature of 173°C and the return profile for 66A-5 was equal to 66-5 when determining the field-averaged performance. The profiles presented in Figure 5 are the field-averaged, normalized returns much like the curves presented in the ideal example (Figure 4C).

The general shape of the tracer profile resembled a single CSTR pass (Figure 1A), which was unique across the assessed Basin and Range geothermal fields, which more commonly ranged from 1.5 to 3. The best fit parameters for the TiS model were: τ_c = 36.08d, τ_p = 2.937 d, n = 1.001, and r = 0.2377. The deconvolution techniques provided similar tracer mass return profiles through early time, and both asymptotically approached some value. The MoM deconvolution converged to ~0.26 due to the higher tail concentrations while the TiS model converged to r, 0.2377. Note the difference between the methods for the converged value is less in the field example than the ideal example because the degree of recycling was less, so the second and subsequent recycle loops were less impactful.

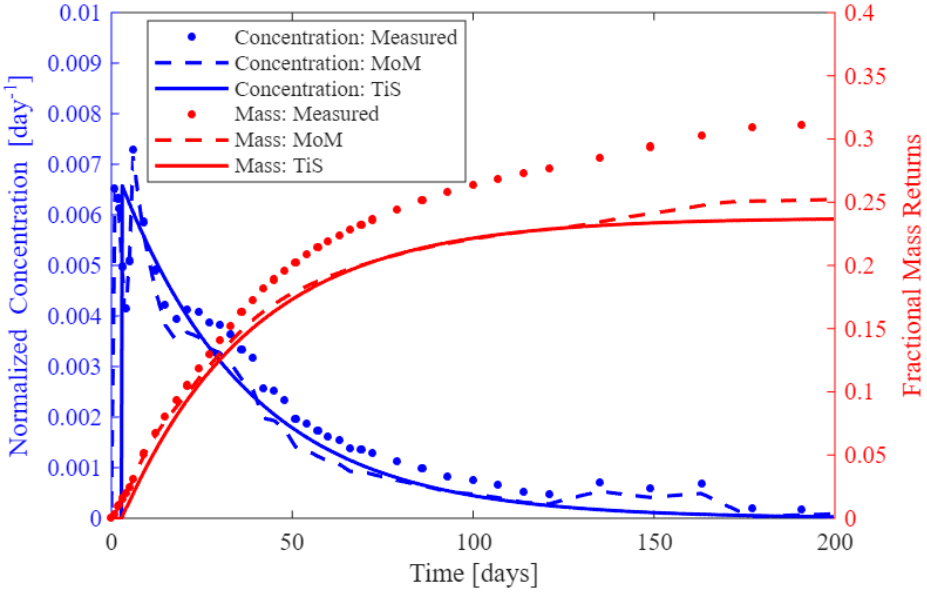

Figure 5: Field-averaged tracer results from a Tuscarora study in 2020 (Kluge, 2025). The curves in blue (left axis) represents normalized concentrations of units [day^{-1}] and the red curves (right axis) represents fractional mass returns.

5. TEMPERATURE EFFECT

One of the primary objectives of tracer studies is to evaluate how reinjection returns may affect geothermal production temperatures. The amount of tracer returns, r, tends to indicate the magnitude of the impact, while the residence times, τ, show how fast the change will happen. The most accurate energy balance for the system would include coupled, 3-D, unsteady differential equations of the reservoir brine and rock with heat transfer between them and an assumed boundary condition for the rock. Following the tank model of the reservoir (Figure 2), a simplified pair of differential equations for the reservoir and rock can be written as

$$mC_p \frac{dT}{dt} = r\dot{m}C_pT_{inj} + (1-r)\dot{m}C_pT_{up} - \dot{m}C_pT + hA(T_r - T) \tag{11}$$

$$m_rC_{p,r} \frac{dT_r}{dt} = -hA(T_r - T) \tag{12}$$

where m is the mass of brine in the reservoir (between injection and production), $\dot{m}$ is the mass rate being produced, C_p is the specific heat of water, h is the heat transfer coefficient, A is the contact area between the brine and reservoir rock, T_{inj} refers to the injection temperature, T_{up} is the resource upflow temperature, which is assumed constant, and the r subscript refers to the reservoir rock. Parameters with no subscript refer to the homogenous space between injection and production.

The coupling with the reservoir rock of unknown size, surface area, and heat transfer coefficient still complicates evaluation for the simplified model, so first, the general decline shape and long-term temperatures were investigated. At infinite time, the rock temperature will approach T, so the convective term can be removed. The remaining terms are representative of the brine from the tracer study. A step-rate disruption associated with reinjection temperature can be introduced to the transfer functions see how the temperature is affected purely by cold injection sweeping through the system and neglecting heat transfer with the rock. The general trends are shown in Figure 1B and would reach a steady temperature on the order of months based on typical geothermal tracer tests. The asymptotic temperature can be estimated as

$$T(t \to \infty) = rT_{inj} + (1 - r)T_{up} \tag{13}$$

Both T_{inj} and T_{up} are assumed to be constant. This asymptotic temperature seems to represent all investigated geothermal fields, meaning none of them have reached it, even for long operating fields like Beowawe (~40 years). The fields close to their asymptotic temperature underwent tapering temperature declines rates and the fields far from the asymptotic temperatures tended to have near linear decline rates; however, the time scale of reaching the temperature is poorly predicted by this approach since it ignores the heat transfer between the reservoir rock and the reinjection brine.

Rather than evaluate the coupled system with unknown h, A, and m_r, it was hypothesized that the CSTR residence time can be scaled by some parameter to better match the observed temperature decline rates and estimate the influence of the heat in place. Tracer studies from various liquid-enthalpy, high permeability fields including Don A. Campbell, Jersey Valley, McGinness Hills, Neal Hot Springs, Platanares, Tungsten Mountain, and Tuscarora were used to try to develop a correlation. Near fully specified tracer tests from each of the fields were analyzed like Tuscarora and a scale factor was selected to best represent the temperature and decline at the time of the tracer test. The investigated correlations included simple transformations or proportions of various parameters including field flow rates, produced volumes, TiS parameters, and best-fit 1-D convective-diffusion model parameters (Horne, 1985). The strongest correlation is represented as the ratio between time allocated to PFR vs. CSTR multiplied by 1030 (Eq. 14); however, this correlation is still being investigated and tends to overestimate the scaling factor depending on how cooled the rock was during the tracer test.

$$Scale\ Factor = 1030\frac{\tau_p}{n * \tau_c} \tag{14}$$

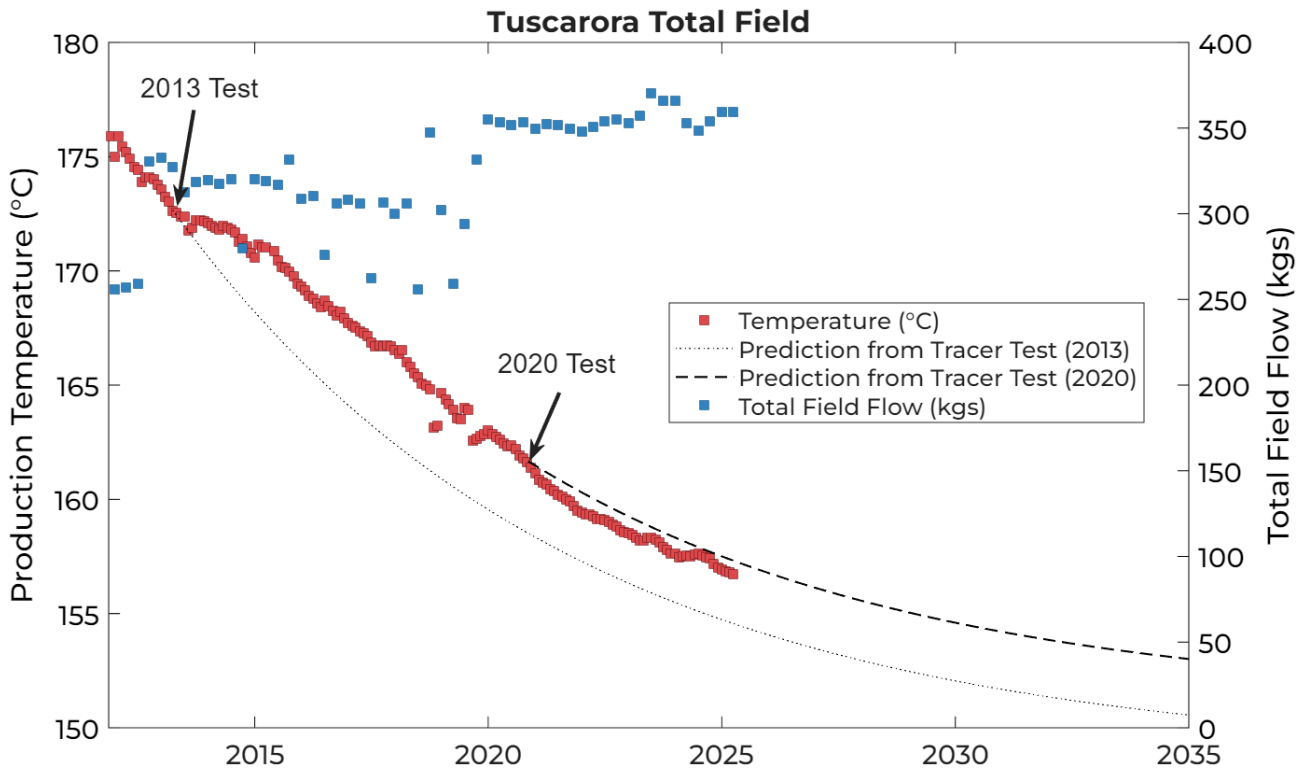

Figure 6: Tuscarora temperature forecasts from 2013 and 2020 tracer forecasts using the best fit TiS model and the scaling factor determined from Eq. 14. The temperature forecasts were shifted through time to align with the temperature at the start of the tracer test.

Figure 6 shows the temperature forecasts from the two Tuscarora tracer studies where the CSTR time was scaled using the correlation estimate. The correlation was able to realistically represent other trained data of geothermal systems with short operating histories, but it has been unsuccessful at estimating the scale factor for tests conducted on fields with longer operating histories, like Beowawe. Generally, the scaling factor for the tracer tests conducted for older fields was a lesser value as the pathway from injection to production was cooled and provides less thermal recharge. In Figure 6, the forecast for the second tracer study had a slightly overscaled decline rate as well, and a better forecast could have been obtained by selecting a lesser scale factor.

There is an important factor not accounted for in Eq. 14 that is related to how cooled the rock is at the time the tracer test, which would decrease the value. Estimating this factor as the age of the geothermal plant was unsuccessful and time when the geothermal plant was offline complicated the correlation. Regardless, an estimated temperature forecast for the resource can be determined using data acquired from a tracer test and an assumed upflow temperature. The residence times or return times can help estimate the rate of temperature decline for the resource, while the recycling fraction, or deconvoluted tracer returns can give an estimate to the magnitude of decline expected from injection returns.

6. CONCLUSIONS

Tracer studies are a pivotal test to assess how reinjection will cool a geothermal resource over time. In this paper, various approaches to estimate a deconvoluted, single-pass tracer profile were discussed. The CSTR in Series model was introduced to aid the deconvolution from continuous and cross-injector recycling using Laplacian transfer functions. The main parameters of the CSTR in Series model include the number of CSTRs, residence times, and the recycling fraction. The residence times can give an estimate at how rapidly the temperature will decline and the recycling fraction, or cumulative single-pass tracer returns, indicates the magnitude of the temperature decline associated with reinjection.

The second half of the paper introduces a concept to create a temperature forecast based on the results of a tracer test without rigorous numerical model calibrations. A step-rate disruption to the transfer functions determined from the tracer tests can provide a forecast how production temperatures will decline for the current injection strategy; however, it requires a time-scaling coefficient to better account for heat in place from the reservoir rock. A correlation trained on tracer tests during the early operating years of geothermal plants is provided to scale the residence times and improve the temperature forecasts; however, there is a pronounced, unaccounted factor associated with the operable age of the geothermal facility, so manually selecting a scale factor to represent the temperature and decline rate during the tracer test may provide better production temperature forecasts.

ACKNOWLEDGEMENTS

The authors would like to thank Ormat Technologies for access to a wide spread of tracer studies across various fields and the permission to publish on these data.

REFERENCES

Abate, J., and Whitt, W.: A Unified Framework for Numerically Inverting Laplace Transforms, INFORMS Journal of Computing, 18.4, (2006): 408-421.

Benoit, D.: Injection Driven Restoration of the Beowawe Geothermal Field, Geothermal Resources Council Transactions, 21, (1997).

Benoit, D.: Large Volume Geothermal Injection in Nevada, GRC Transactions, 41, (2017).

Fogler, S.H.: Elements of Chemical Reaction Engineering, 4th Edition, Pearson, (2014). Ch 14.

Folsom, M., Libbey, R., Feucht, D., Warren, I., and Garanzini, S.: Geophysical Observations and Integrated Conceptual Models of the San Emidio Geothermal Field, Nevada, Workshop on Geothermal Reservoir Engineering, 46, (2020).

Forest, R.T., Johnson, S.E., and Johnson, S.D.: An Injection Turnabout Success at Stillwater, Nevada, Geothermal Resources Council Transactions, 19, (1995).

Horne, R.N., Gilardi, J., and Bouett, L.: Dispersion of Tracers in Fractures – Experiments at Stanford University, Proceedings of NZ Geothermal Workshop, 7, (1985).

Kluge, E., Ferguson, C., Reynolds, Z., Motley, C., Libbey, R., Murphy, J., and Akerley, J.: Updated Conceptual Model and Reservoir Assessment of the Tuscarora Geothermal Field: Over a Decade of Renewable Power Generation, GRC Transactions, 49, (2025).

Levenspiel, O.: Chemical Reaction Engineering, 2nd Edition, John Wiley and Sons, (1972), Ch. 9.

Robinson, B.: Determining the True Residence Time Distribution Curve of Phase I System, memorandum, Los Alamos National Laboratory, (1982).

Romagnoli, J.A., and Palazoglu A.: Introduction to Process Control, 2nd Edition, CRC Press, (2012).

Rose, P.E., Benoit, W.R., and Kilbourn, P.M.: The application of the polyaromatic sulfonates as tracers in geothermal reservoirs, Geothermics, 30.6, (2001): 617-640.

Sajkowski, L., Seward, T.M., Mountain, B.W., and Marynowski, L.: 1-5-Napthalene disulfonate stability and breakdown kinetics in aqueous solutions under geothermal conditions

Shook, G.M.: A Simple, Fast Method of Estimating Fractured Reservoir Geometry from Tracer Tests, Geothermal Resources Council, 27, (2003), 407-411.

Shook, G.M.: Tracers and Tracer Testing: Design, Implementation, and Interpretation Methods, Idaho National Engineering and Environmental Lab, INEEL/EXT-03-01466, (2004).

Shook, G.M.: A Systematic Method for Tracer Test Analysis: An Example Using Beowawe Tracer Data, Proceedings, Workshop of Geothermal Reservoir Engineering, 30, (2005).

Shook, G.M., and Forsmann J.H.: Tracer Interpretation Using Temporal Moments on a Spreadsheet, Idaho National Labs, INL/EXT-05-00400, (2005).

Tester, J.W., Robinson, B.A., and Ferguson, J.H.: Inert and Reacting Tracers for Reservoir Sizing in Fractured, Hot Dry Rock Systems, Workshop on Geothermal Reservoir Engineering, 11, (1986).